JOURNAL OF MATERIALS SCIENCE 32 (1997) 701–711

Stress transfer in the fibre fragmentation test

Part III *Effects of interface debonding and matrix yielding*

JANG-KYO KIM
Centre for Advanced Engineering Materials, and Department of Mechanical Engineering, Hong Kong University of Science and Technology, Clear Water Bay, Hong Kong

The micromechanics of stress transfer is presented for the fibre fragmentation test of microcomposites containing debonded fibre–matrix interface and yielded matrix at the interface region. Results from the parametric study are discussed for carbon fibre composites containing epoxy and polyetheretherketone (PEEK) matrices, representing respectively typical brittle debonding and matrix yielding behaviour at the interface region. The stress transfer phenomena are characterized for the two interface failure processes. The sequence of interface failure and fibre fracture as a function of applied stress are also identified. Maximum debonded and yielded interface lengths are obtained above which a fibre will fracture into smaller lengths. There are also threshold fibre fragment lengths above which fibre will fracture without interface debonding or matrix yielding. The applied stresses for these conditions are governed by three strength properties of the composite constituents, namely interface shear bond strength, matrix shear yield strength and fibre tensile strength for given elastic constants of the fibre and matrix, and the geometric factors of the microcomposite. The ineffective length, a measure of the efficiency of stress transfer across the fibre–matrix interface, is shown to strongly depend on the extent to which these failure mechanisms take place at the interface region.

1. Introduction

Characterization of the stress transfer across the fibre–matrix interface has received significant attention, especially using the fibre fragmentation test geometry which has become one of the most popular means of measuring fibre–matrix properties [1, 2]. The fibre fragmentation test gives information on the basic damage modes taking place in multiple fibre composites subjected to uniaxial tension. The primary functions of the interface are to allow efficient stress transfer between the fibre and matrix, and to protect the reinforcing fibres in adverse environments encountered during the manufacturing processes and in service. Optimal mechanical properties of a fibre composite are strongly related to the efficiency of stress transfer across the interface. Feillard *et al.* [3] have recently presented a comprehensive review on the current status of theoretical understanding of the fibre fragmentation test.

Following our previous theoretical study on interface debonding processes in fibre pull-out of single and multiple fibre composites [4, 5], the micromechanics of stress transfer is analysed in the fibre fragmentation test geometry [6, 7]. Depending on the interface properties and fibre tensile strength for given elastic properties of the fibre and matrix, three distinct interface conditions are identified, namely full bonding, partial debonding and complete debonding. The effects of interactions between neighbouring fibres on fibre fracture and interface debonding are also evaluated in multiple fibre composites using the three cylinder composite model [8].

Apart from the clear-cut interface debonding behaviour which has been considered previously, the matrix material surrounding the fibre may yield and plastically deform if the interface bond strength is greater than the matrix shear strength as in many polymer and metal matrix composites [9–13]. Laser Raman spectroscopy studies [14, 15] have shown that the maximum interface shear stresses correlate closely with the shear yield strength of the matrix materials of different chemical structures, and suggested that shear yielding is an important failure mechanism at the interface region. The thin layers and particles of resin adhering to the fibre surface which are often observed in scanning electron microscopy of fracture surfaces [16, 17] further testify to the above failure mechanisms.

The concepts of ineffective length and critical transfer length of a broken fibre under tensile load were developed [18, 19] in order to describe the effect of stress decay towards the fibre ends. The ineffective length was originally defined as the portion of the fibre in which the average axial stress is greater than some fraction of the stress at the far-field of infinitely long fibres. If the fibres are shorter than the ineffective

0022–2461

length then they are considered to be ineffective in reinforcing the composites. In a similar concept, the critical transfer length is defined as the shortest fibre length along which the axial stresses build up sufficiently to fracture the fibre. From experiments, a critical transfer length is taken from the mean value of fibre fragment lengths determined after further substantial increment in the applied stress leads to no additional fibre fragmentation.

It has been proposed both experimentally [20–25] and theoretically [6, 7, 26, 27] that in contrast to the conventional opinion of either full bonding or complete debonding/matrix yielding there is an intermediate case in which both bonded and debonded/yielded interfaces are present simultaneously during the fibre fragmentation process of some polymer matrix composites. This in turn determines the critical transfer length. A large volume of evidence is available, for example see references [28–35], to show that these characteristic lengths provide information about varying efficiencies of stress transfer as a result of fibre surface treatment/interlayer coating and environmental degradation. The temperature dependence of the shear yield strength of a matrix material at the interface region also greatly affects the critical transfer length [36–38]. The functional dependence of critical transfer length or ineffective length on the Young's modulus ratio of the fibre to the matrix, E_f/E_m, has also been studied [39–41]. The critical transfer length is also found to be dependent on the reversible work of adhesion between the composite constituents [42, 43], matrix viscosity [44] and cohesive energy ratio of the fibre to the matrix [45]. Nevertheless, whether an explicit treatment of the ineffective length or the critical transfer length is necessary to calculate the absolute values of useful interface properties is still questionable.

In the present paper, a theoretical analysis of matrix yielding at the interface region is developed, and the criteria for partial matrix yielding and fibre fracture are evaluated for the fibre fragmentation test geometry. Incorporating the analysis [6] previously developed for composites with interfacial debonding, comparisons are made of the criteria and the associated stress fields for the three opposing failure mechanisms, namely, fibre fracture, interface debonding and matrix yielding. A special emphasis is placed on the evaluation of the ineffective lengths, as a measure of the efficiency of stress transfer, which are predicted from the models developed in the current analyses.

2. Micromechanics analysis

2.1. Solutions for the stress fields

The geometry and the governing conditions of the shear-lag model are essentially the same as those adopted in our previous analyses [6, 7]. Fig. 1 shows a cylindrical model which is symmetric about the fibre axis $r = 0$ and the mid-plane at $z = 0$. A single fibre of total length $2L$ with a debonded or yielded interface length l at both its ends is located at the centre of a cylindrical matrix material. When a tensile stress, σ, is applied to the ends of a matrix cylinder, the stress

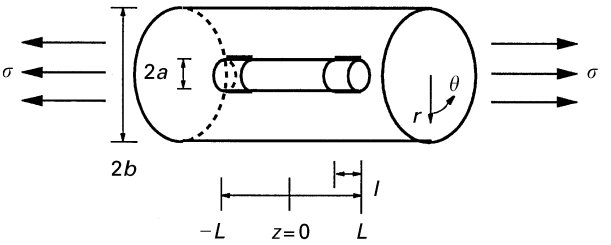

Figure 1 A schematic drawing of the fibre fragmentation model with partially debonded or yielded interfaces at its ends.

is transferred to the fibre across the fibre–matrix interface. For the cylindrical coordinate (r, θ, z), the solutions for the fibre axial stress (FAS) and interface shear stress (ISS) in the bonded region ($-(L-l) \leqslant z \leqslant (L-l)$) are derived [6]:

$$\sigma_f^z(z) = \frac{1+\gamma}{\alpha+\gamma}\left[1 - \frac{\cosh(\beta_2 z)}{\cosh[\beta_2(L-l)]}\right] \times \sigma + \frac{\cosh(\beta_2 z)}{\cosh[\beta_2(L-l)]}\sigma_1 \quad (1)$$

$$\tau_i(z) = \frac{a\beta_2}{2}\left[\frac{1+\gamma}{\alpha+\gamma}\sigma - \sigma_1\right]\frac{\sinh(\beta_2 z)}{\cosh[\beta_2(L-l)]} \quad (2)$$

where

$$\beta_2^2 = \left[\left(\frac{b}{a}\right)^2 - 1\right]\left(1 + \frac{\alpha}{\gamma}\right)\Big/ a^2(1+\gamma) \times \left[\left(\frac{b}{a}\right)^4 \ln\left(\frac{b}{a}\right) - \frac{1}{2\gamma^2} - \frac{1}{4\gamma}\left(\frac{b^2}{a^2}+1\right)\right] \quad (3)$$

The Young's modulus ratio of the matrix to the fibre, $\alpha = E_m/E_f$, and the volume ratio of the fibre to the matrix, $\gamma = a^2/(b^2 - a^2)$. σ_1 is the FAS at the boundary between the bonded and debonded (or yielded) interface regions. For the fully bonded interface, the above equations are still valid except for $\sigma_1 = 0$ and $l = 0$.

Based on the maximum shear stress criterion, it is assumed here that either interfacial debonding or matrix yielding occurs when the maximum shear stress at the fibre–matrix interface reaches the lower strength value of the two composite constituents. If the interface shear strength, τ_b, is significantly greater than the apparent matrix shear yield strength, τ_{my}, yielding takes place in the matrix material near the interface in preference to interface debonding, and *vice versa*. Work-hardening is neglected for the elastic–perfectly plastic matrix material in the case of matrix yielding. For simplicity, the thickness of the material involved in these failure mechanisms are regarded as being infinitely thin. It is also assumed that the above failure mechanisms are mutually exclusive, and that only one failure mechanism can occur for a given set of properties of the composite constituents.

The solutions for the major stress fields are obtained [6] for the debonded regions, ($-L \leq z \leq -(L-l)$ and $(L-l) \leq z \leq L$):

$$\sigma_f^z(z) = \frac{B_3}{B_2}[D_1\exp(m_2 z) + D_2\exp(m_1 z)] + \sigma_1[D_3\exp(m_2 z) + D_4\exp(m_1 z)] \quad (4)$$

$$\tau_i(z) = -\frac{a}{2}\left[\frac{B_3}{B_2}[m_2 D_1 \exp(m_2 z) + m_1 D_2 \exp(m_1 z)] + \sigma_1[m_2 D_3 \exp(m_2 z) + m_1 D_4 \exp(m_1 z)]\right] \quad (5)$$

where the debond crack tip stress, σ_1, at the boundary between the bonded and debonded regions is given by:

$$\sigma_1 = \frac{1+\gamma}{\alpha+\gamma}\sigma - \frac{2\tau_b}{a\beta_2}\coth[\beta_2(L-l)] \quad (6)$$

The non-dimensional coefficients D_1, D_2, D_3, D_4, m_1, m_2, B_1 and B_2 are presented in Appendix A. The corresponding solutions for the stress components in the yielded regions, are obtained as;

$$\sigma_f^z(z) = \frac{2}{a}\tau_{my}(L-z) \quad (7)$$

$$\tau_i(z) = \tau_{my} \quad (8)$$

where the FAS at the boundary between the bonded and yielded region, σ_l, is given by:

$$\sigma_l = \frac{2l}{a}\tau_{my} \quad (9)$$

2.2. Conditions for interface debonding, matrix yielding and fibre fragmentation

Based on the solutions for the major stress components, the relevant criteria for interface debonding and matrix yielding at the interface and fibre fragmentation are obtained. The conditions required to satisfy the interface states with full bonding and partial interface debonding and partial matrix yielding are also identified in terms of the relationship between the applied stress and the properties of the constituents. The stress applied to the matrix at the remote ends, $\sigma = \sigma_{od}$, for debond crack propagation is given:

$$\sigma_{od} = \frac{\frac{2n_3}{a\beta_2}\tau_b \coth[\beta_2(L-l)] - \alpha v_f(n_1+\lambda)\bar{\sigma}}{(1+\gamma)\left[\frac{n_3}{\alpha+\gamma} + v_m n_1\right]} \quad (10)$$

where n_1 and n_3 are given in Appendix A. $\bar{\sigma}(=-q/\omega k)$ is the asymptotic debond stress for a long fibre length, and $\lambda(=2\mu k/a)$ is the reciprocal length giving the effective frictional stress transfer [4]. The interfacial properties at the debonded interface are, q_0 which is the residual fibre clamping stress and μ the coefficient of friction. The corresponding external stress applied to the matrix, $\sigma = \sigma_{oy}$, for matrix yielding at the interface region is obtained:

$$\sigma_{oy} = \frac{\alpha+\gamma}{1+\gamma}\frac{2\tau_{my}}{a}\left[l + \frac{1}{\beta_2}\coth[\beta_2(L-l)]\right] \quad (11)$$

The fibre fragmentation criterion chosen here is such that when the applied stress is sufficiently high to cause the maximum FAS to reach the local tensile strength, the fibre fractures at the centre [6, 7]. The average fibre tensile strength of a fibre segment of length, $2L$, is given, based on the Weibull probability of failure as;

$$\sigma_{TS}(2L) = \sigma_{TS}(2L_g)\left(\frac{L_g}{L}\right)^{1/m} = \sigma_u(2L_g)^{-1/m}\Gamma\left(1+\frac{1}{m}\right)\left(\frac{L_g}{L}\right)^{1/m} \quad (12)$$

where m and σ_u are the Weibull modulus and the scale factor, and Γ is the gamma function. Thus, the external stress required for fibre fragmentation, $\sigma = \sigma_{of}$, is derived:

$$\sigma_{of} = \frac{\alpha+\gamma}{1+\gamma}\frac{\sigma_{TS}\cosh[\beta_2(L-l)] - \sigma_l}{\cosh[\beta_2(L-l)] - 1} \quad (13)$$

for the partially debonded interface, and

$$\sigma_{of} = \frac{\alpha+\gamma}{1+\gamma}\frac{\sigma_{TS}\cosh[\beta_2(L-l)] - \frac{2l}{a}\tau_{my}}{\cosh[\beta_2(L-l)] - 1} \quad (14)$$

for the yielded matrix at the interface region. The solution of the corresponding external stress for the fully bonded interface can be obtained from Equation 13 or Equation 14 for $l = 0$ and $\sigma_l = 0$:

$$\sigma_{of} = \frac{\alpha+\gamma}{1+\gamma}\frac{\sigma_{TS}\cosh(\beta_2 L)}{\cosh(\beta_2 L) - 1} \quad (15)$$

The fibre–matrix interface remains fully bonded as far as the interface shear stress governed by Equation 2 is smaller than either τ_b or τ_{my}. Therefore, the governing condition for the full interface bonding is obtained:

$$\tau_b, \tau_{my} > \frac{a\beta_2}{2}\frac{\sigma_{TS}\sinh(\beta_2 L)}{\cosh(\beta_2 L) - 1} \quad (16)$$

It should be noted here that whether interfacial debonding or matrix yielding continues, or fibre fracture occurs depends on the relative magnitudes of the stresses required for these failure processes, σ_{of}, σ_{oy} and σ_{of}. Further, the relationship between the interface bond strength, τ_b, and the instantaneous debond length obtained at the moment of fibre fragmentation is also derived by combining Equations 6, 10 and 13:

$$\tau_b = \frac{a\beta_2}{2}\frac{[n_3 + v_m n_1(\alpha+\gamma)]\sigma_{TS} + \alpha v_f(n_1+\lambda)\bar{\sigma}}{n_3\coth[\beta_2(L-l)] - [n_3 + v_m n_1(\alpha+\gamma)]\operatorname{cosech}[\beta_2(L-l)]} \quad (17)$$

for the partially debonded interface model. Similarly, Equations 9, 11 and 14 give the corresponding relationship between the matrix shear strength, τ_{my}, and the yield length:

$$\tau_{my} = \frac{a\sigma_{TS}}{2l + \frac{2}{\beta_2}\frac{\cosh[\beta_2(L-l)] - 1}{\sinh[\beta_2(L-l)]}} \quad (18)$$

for the partially yielded interface model.

Based on the interface debond, matrix yield and fibre fragmentation criteria given by Equations 10–15,

the solutions for the mean fibre fragment length, $2L$, is derived as a function of the applied stress, σ_{of}.

$$2L = \frac{2}{\beta_2}\cosh^{-1}\left[\frac{\sigma_{of}}{\sigma_{of} - \frac{\alpha+\gamma}{1+\gamma}\sigma_{TS}}\right] \quad (19)$$

for the fully bonded interface,

$$2L = \frac{2}{\beta_2}\sinh^{-1}\left[\frac{\frac{2\tau_b}{a\beta_2}}{\frac{1+\gamma}{\alpha+\gamma}\sigma_{of} - \sigma_{TS}}\right] + 2l \quad (20)$$

for the partially debonded interface, and

$$2L = \frac{2}{\beta_2}\cosh^{-1} \times\left[\left(\frac{1+\gamma}{\alpha+\gamma}\sigma_{of} - \frac{2l}{a}\tau_{my}\right)\Big/\left(\frac{1+\gamma}{\alpha+\gamma}\sigma_{of} - \sigma_{TS}\right)\right] + 2l \quad (21)$$

for the partially yielded matrix at the interface region.

2.3. Ineffective length

The concept of ineffective transfer length is adopted here to evaluate the efficiency of stress transfer across the interface. The ineffective length, 2δ, is defined as the fibre length necessary to build up a maximum stress equivalent to a fraction, ϕ, of that for an infinitely long fibre [46]. Since the fibre axial stress (FAS) is symmetric about the fibre centre, the stress ratio, ϕ, can be written as:

$$\phi = \frac{\sigma_f(L-\delta)}{\sigma_f(0)_{L\to\infty}} \quad (22)$$

By combining Equation 22 with the relevant solutions for the FAS given by Equations 1, 6 and 9, the solutions for the stress ratio are derived in Appendix B. Thus, half the ineffective length, δ, is expressed as:

$$\delta = \frac{1}{\beta_2}\cosh^{-1}\left[\frac{1+(1-\phi)^2}{2(1-\phi)}\right] \quad (23)$$

for the fully bonded interface,

$$\delta = l - \frac{1}{\beta_2}\ln\left[\left[\frac{a\beta_2}{2\tau_b}\frac{1+\gamma}{\alpha+\gamma}(1-\phi)\sigma + \frac{\phi}{\sinh[\beta_2(L-l)]}\right]\right] \quad (24)$$

for the partially debonded interface, and

$$\delta = l - \frac{1}{\beta_2}\ln\left[\left[(1-\phi)(l\beta_2+1)\right]\right] \quad (25)$$

for the partially yielded interface. As for the mean fibre fragment lengths given by Equations 20 and 21, the ineffective lengths for the partially debonded and yielded interfaces consist of both the bonded and failed interface lengths. It is noted that Equation 23 is essentially the same as that proposed originally by Rosen [18] and its modified version [47] for elastic stress transfer in a fully bonded interface, except for the coefficient β_2 which is different in the respective models depending on the effective fibre volume fraction. Furthermore, it is worth mentioning that neither the fibre tensile strength nor the interface properties come into play in determining the effective lengths in the models for elastic stress transfer.

3. Results

Specific results are calculated in order to highlight the trends exposed by the equations presented in the preceding sections. Model carbon fibre composites are employed in the present study which contain two different matrix materials: epoxy and polyetheretherketone (PEEK). These matrix materials are considered to show typical brittle debonding and matrix yielding behaviour which take place, respectively, at the interface regions with the carbon fibres. The mechanical properties used for the calculations are $E_f = 230$ GPa and $\nu_f = 0.2$ for the carbon fibre; $E_m = 3.0$ GPa, $\nu_m = 0.4$ and $\tau_b = 72.7$ MPa for the epoxy matrix; and $E_m = 3.8$ GPa, $\nu_m = 0.4$ and $\tau_{my} = 46$ MPa for the PEEK matrix, unless otherwise varied. The interfacial properties at the debonded region are: $q_0 = -10$ MPa and $\mu = 1.5$. The Weibull statistics for the fibre tensile strength are presented elsewhere [6].

3.1. Stress transfer in the composite constituents

The FAS and ISS distributions normalized with applied stress for the partially debonded and yielded interfaces are presented along the fibre length in Figs 2 and 3. Since a constant stress is applied to the model composites with an identical total fibre length, different debond and yield lengths are shown for different interface properties, τ_b and τ_{my}. It is noted that the maximum FAS values obtained in the central region of the fibre are insensitive to the τ_b and τ_{my} values studied (Figs 2a and 3a). The FAS strongly decreases towards zero near the failed interface region. The sensitivity of the decaying FAS values on the interface properties, τ_b and τ_{my}, greatly affects the ineffective length, a measure of the efficiency of stress transfer across the interface. Higher τ_b and τ_{my} values resulted in higher FAS values at a given distance from the fibre end, giving rise to short ineffective lengths, that will be detailed later. A shorter ineffective length corresponds to a more efficient stress transfer.

The interface shear stress (ISS) fields for the debonded interface are discontinuous with varying stress drops at the boundary between the bonded and debonded regions. In the debonded region, the interface stress increases towards the fibre ends due to the differential Poisson contraction between the fibre and matrix (Fig. 2b). In general, a high frictional shear stress which is a result of the high coefficient friction, μ, and/or high residual fibre clamping stress, q_0, promotes efficient stress transfer at the debonded region, effectively reducing the ineffective length [21]. Contrary to the rising ISS at the debonded interface, the constant values at the yielded interface region are identical to the τ_{my} values used for the calculations, directly reflecting the boundary conditions (Fig. 3b). However, a higher τ_b or τ_{my} value commonly resulted

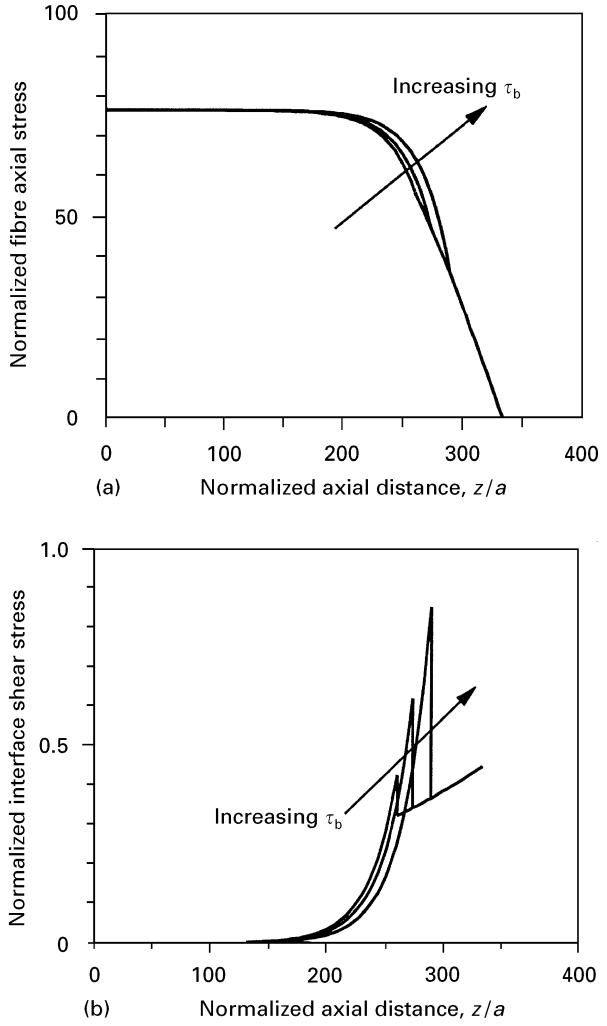

Figure 2 (a) Fibre axial stress and (b) interface shear stress distributions normalized with external stress along the fibre axis for partially debonded interface. Interface shear bond strength, $\tau_b = 50$, 72.7 and 100 MPa.

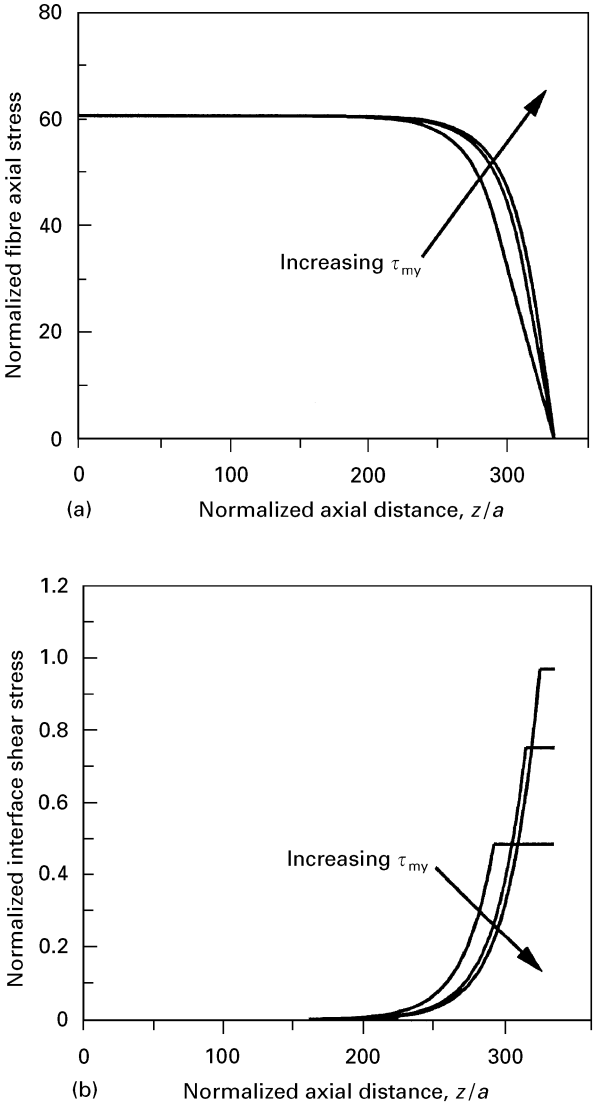

Figure 3 (a) Fibre axial stress and (b) interface shear stress distributions normalized with external stress along the fibre axis for partially yielded interface. Matrix shear yield strength, $\tau_{my} = 30$ MPa, 46 and 60 MPa.

in shorter debonded and yielded lengths at a given external stress and a fibre length.

3.2. Interface debonding, matrix yielding and fibre fragmentation

The criteria for initial interface debonding or matrix yielding based on Equation 16 are summarized in Fig. 4 which displays the critical values of τ_b or τ_{my} for these failure mechanisms to take place at given fibre lengths. It is noted that the curve increases parabolically towards an infinite τ_b or τ_{my} value as the mean fibre fragment length decreases. This suggests that interface debonding or matrix yielding is relatively easy when the fibre is sufficiently long, and becomes increasingly more difficult as fibre fragmentation proceeds. The slight difference between the two τ_b and τ_{my} curves results from the difference in the matrix Young's moduli values used for the calculations which affects the magnitudes of the coefficients β_2 in Equation 3.

Furthermore, the dependence of the maximum debond and yield lengths on the interface properties and fibre length before fibre fragmentation initiates is presented in Fig. 5. It is shown that for given interface properties, a longer fibre length results in shorter maximum debond and yield lengths before fibre fractures due to the strong dependence of the average fibre tensile strength on the fibre length as suggested in Equation 12. If the interface shear strength is greater than a critical value then the interface does not fail at all. These critical values are obtained: $\tau_b = 98.6$, 82.1 and 68.4 MPa, and $\tau_{my} = 106.6$, 88.7 and 73.9 MPa for $2L = 1$, 2 and 4 mm, respectively, which can also be determined from Fig. 4. As expected, both the maximum debond and yield lengths increase with reducing the interface shear properties towards finite values. It is worth noting that only a portion of the fibre length can be debonded even for a negligible shear bond strength, τ_b (Fig. 5a). This observation is considered to be a direct consequence of the larger Poisson contraction of the matrix than the fibre in uniaxial tension. The ISS thereby increases towards the fibre ends from the debond interface boundary, effectively discouraging further debond propagation. In other words, the elastic properties of the composite constituents, together with the interface properties, play an important role in controlling the debond propagation. In

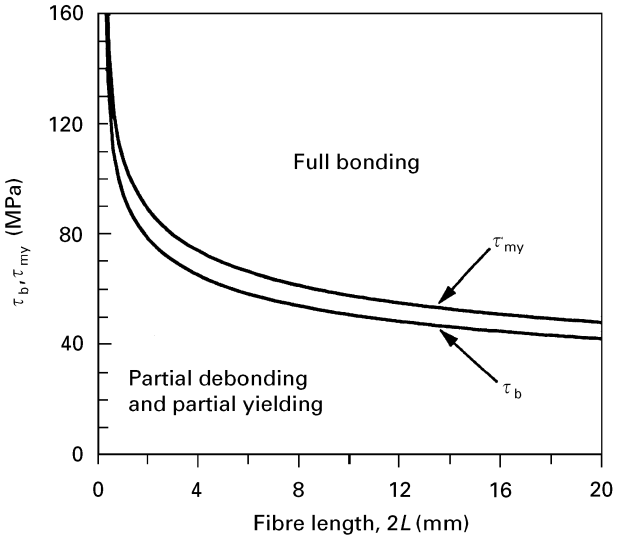

Figure 4 Plots of interface shear bond strength, τ_b, or matrix shear yield strength, τ_{my}, as a function of fibre length showing the regions of full bonding and partial interface debonding or partial matrix yielding.

contrast to the partially debonded interface, interface yielding can be extended virtually over the whole fibre length if τ_{my} is sufficiently low (Fig. 5b). A longer fibre length requires a lower τ_{my} value for full interface yielding.

The relationships between the applied stresses required for interfacial debonding, matrix yielding and fibre fragmentation, σ_{od}, σ_{oy}, and σ_{of}, are obtained from Equations 10, 11, 13 and 15, which are plotted as a function of normalized debond or yield length, l/a, in Figs 6 and 7. A careful examination of these figures allows the sequential failure processes to be identified during the fibre fragmentation test. Fig. 6 suggests that when the fibre is sufficiently long at the initial stage of the test, fibre fragmentation can only occur until the fibre lengths become short enough not to allow further fibre fracture. At this stage, transition of failure process occurs from fibre fragmentation to interface failure because the external stress required for the latter process, σ_{od} or σ_{oy}, is smaller than that for the former process, σ_{of}. The applied stresses required for interface failure, σ_{od} and σ_{oy}, are independent of fibre length for a given set of interface properties, τ_b and τ_{my}. It can be seen that the applied stresses and the corresponding threshold debond and yield lengths before fibre fragmentation resumes increase with decreasing fibre length.

Once the fibre segment lengths become sufficiently short after substantial fibre fragmentation (e.g. $2L = 2$ mm as in Fig. 7), the interface fails. The debond and yield lengths grow until they become threshold values when transition of failure process occurs again from interface failure to fibre fragmentation. The applied stresses, σ_{od} and σ_{oy}, required for initial interface failure as well as the threshold debond and yield lengths before fibre fragmentation resumes are strongly dependent on the interface properties, τ_b or τ_{my}, for a given fibre length. The points where the curves, σ_{od} and σ_{oy}, originate at the abscissa represent the applied stresses required to initiate the respective failure processes, while the intersecting points between the external stresses, σ_{od} and σ_{of} (and σ_{oy} and σ_{of}),

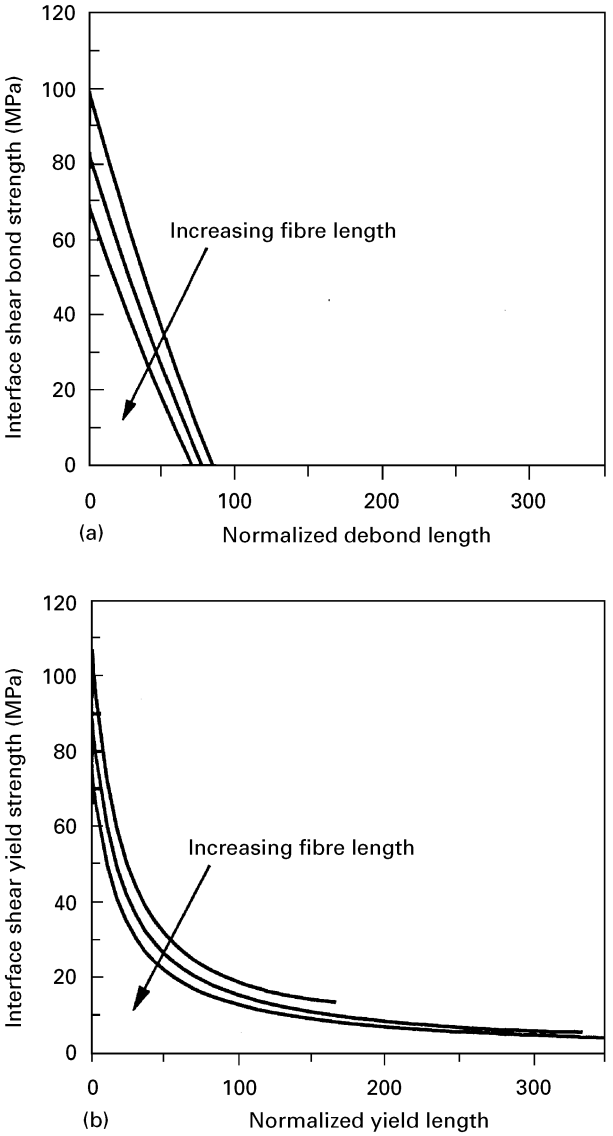

Figure 5 (a) Plots of interfacial shear bond strength, τ_b, and (b) interface matrix yield strength, τ_{my}, as a function of normalized debond or yield length, l/a for varying embedded fibre length $2L$.

represent the transition of failure process from interfacial debonding (or matrix yielding) to fibre fragmentation, or *vice versa*. For example, the applied stresses required for interface failure initiation are obtained: $\sigma_{od} = 30.4$, 44.2 and 60.8 MPa for $\tau_b = 50$, 72.7 and 100 MPa (Fig. 7a); $\sigma_{oy} = 21.0$, 32.2 and 42.0 MPa for $\tau_{my} = 30$, 46 and 60 MPa (Fig. 7b), respectively. The threshold yield length, $(2l)_m = 0.125$, 0.059 and 0.031 mm are also determined for $\tau_{my} = 30$, 46 and 60 MPa and $2L = 2$ mm (Fig. 7b). Once there is substantial debonding or yielding along the interface, fibre fragmentation resumes because the latter process requires a lower applied stress than the former processes at a given fibre length. In contrast to the interface failure processes, the fibre fragmentation process is totally independent of the interface properties as envisaged by one curve for σ_{of} representing the three different interface properties (Fig. 7). An almost constant applied stress, σ_{of}, is shown for fracture of a fibre regardless of its debond or yield length. (The rising or decaying σ_{of} values for long debond or yield length in Figs 6 and 7 only show the trend obtained from the model without practical implications.)

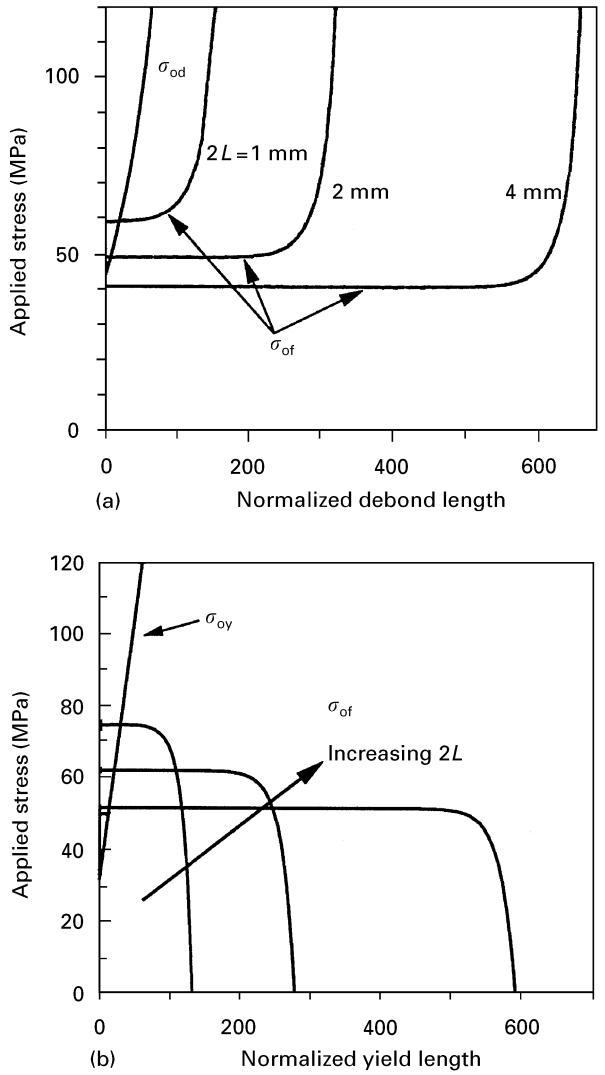

Figure 6 Comparisons of applied stresses required (a) for interface debonding, σ_{od}, and fibre fragmentation, σ_{of}, and (b) for matrix yielding, σ_{oy}, and fibre fragmentation, σ_{of}, as a function of normalized debond (or yield) length, l/a. $\tau_b = 72.7$ MPa and $\tau_{my} = 46$ MPa.

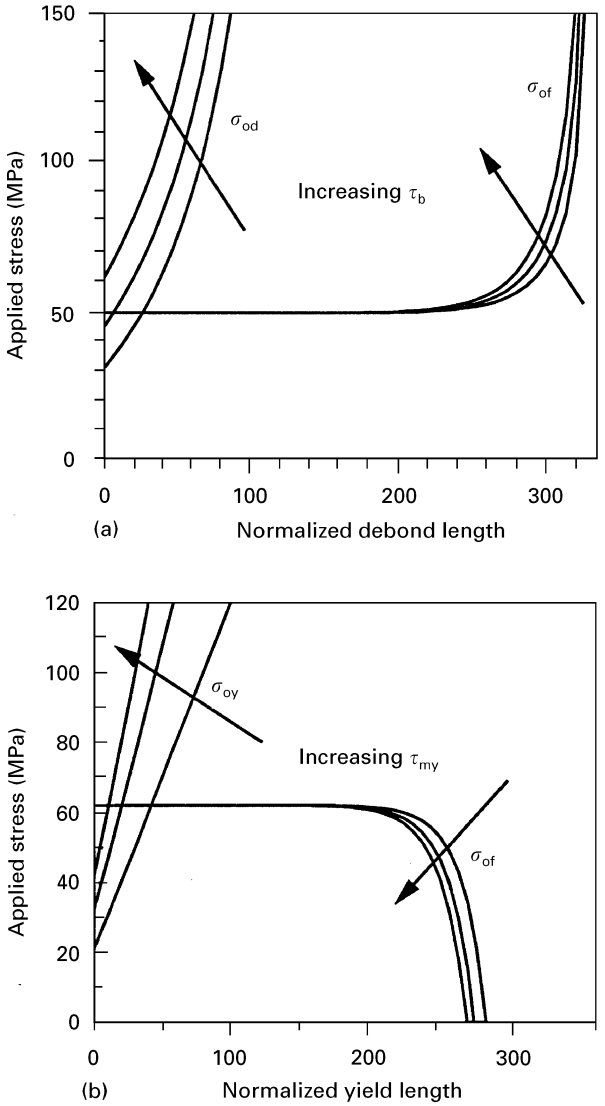

Figure 7 Comparison of applied stresses required (a) for interface debonding, σ_{od}, and fibre fragmentation, σ_{of}, and (b) for matrix yielding, σ_{oy}, and fibre fragmentation, σ_{of}, as a function of normalized debond or yield length, l/a. Fibre length, $2L = 2$ mm.

The progress of interface failure processes is further studied with reference to Fig. 8 where the debond and yield lengths are plotted as a function of applied strain for a given fibre length. Both the debond and yield lengths are shown to increase towards maximum values with applied strain, a higher external strain being required to induce the same extent of interface failure for a high value of τ_b or τ_{my}, which is consistent with the findings from Fig. 7. It is also identified that there are threshold applied strains or stresses below which debonding or yielding does not take place. These values can be directly taken from the intersecting points of the curves with the ordinate, and are identical to those values discussed above with reference to Fig. 6. It is worth noting that the yield length and applied strain have an approximately linear relationship, whose gradient becomes smaller with increasing matrix shear yield strength, τ_{my} (Fig. 8b).

3.3. Ineffective lengths

Based on the discussion presented above, the efficiency of stress transfer across the fibre–matrix interface is summarized in Fig. 9 where the ineffective lengths calculated using Equations 23–25 for a stress ratio $\phi = 0.9$ are compared between the composites with fully bonded, partially debonded and partially yielded interfaces. It is shown that at the initial stage of a fibre fragmentation test in which the whole fibre length is fully bonded with the matrix, the ineffective length is constant. The marginally higher constant ineffective length obtained for the carbon–epoxy system (Fig. 9a) compared to that for the carbon–PEEK system (Fig. 9b) appears to be a direct reflection of the slightly lower matrix Young's modulus value for the former composite than the latter composite. This observation is basically consistent with the previous findings [40, 41] in that the ineffective length or the critical transfer length varies almost linearly with the Young's modulus ratio of the fibre to the matrix, E_f/E_m, in a ln–ln plot. It was also reported that a compliant interlayer present on the fibre surface gives rise to the critical transfer length [33], which in turn promotes large interface debonding and subsequent fibre pull-out in transverse fracture of epoxy matrix composites containing such fibres [48].

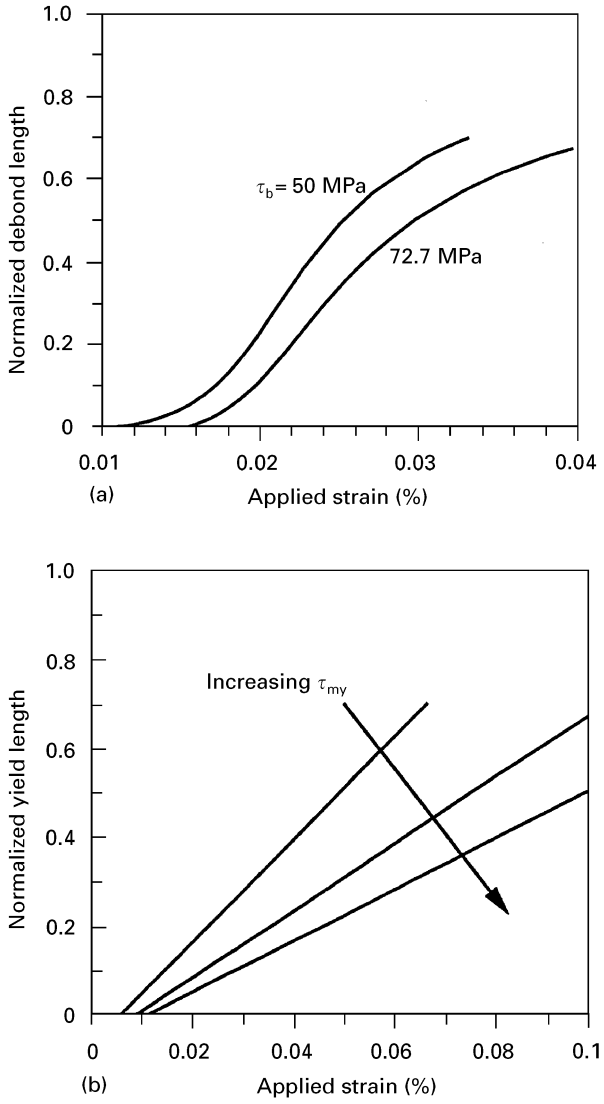

Figure 8 Variation of normalized debond or yield length, l/L, and with applied strain for (a) the partially debonded interface and (b) the partially yielded interface.

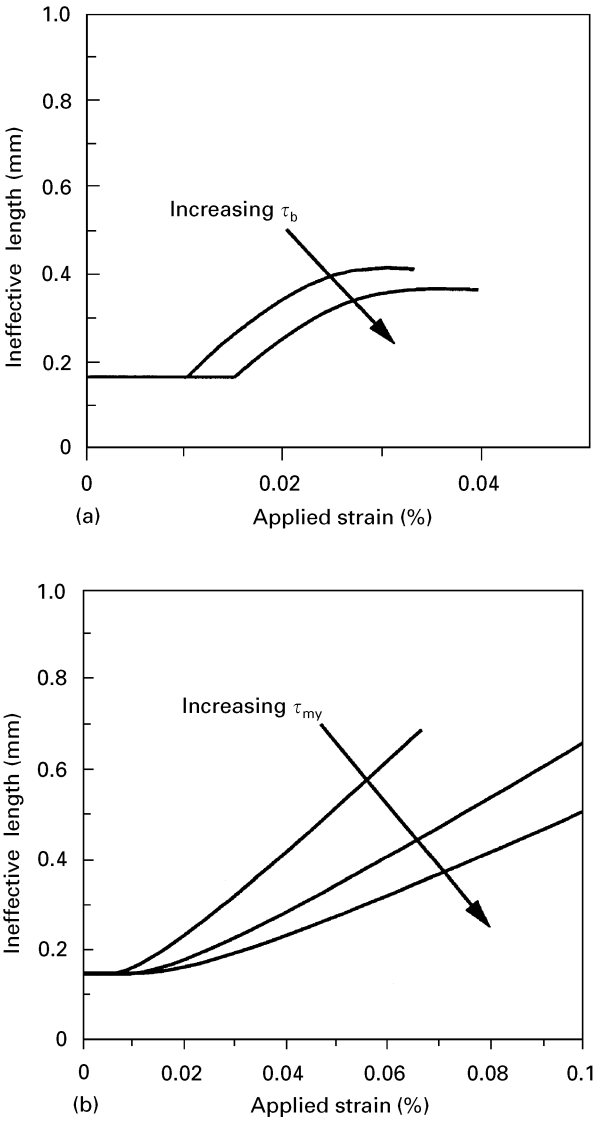

Figure 9 Variation of normalized ineffective length, δ/a, with applied strain for (a) the partially debonded interface and (b) the partially yielded interface.

With a further increase in the applied strain, there are transition points where the ineffective lengths deviate from being constant. These threshold applied strains are found to increase with increasing τ_b and τ_{my}, as shown in Figs 7 and 8. The ineffective lengths for both the debonded and yielded interfaces increase steadily with applied strain above the threshold values as a result of increased debond and yield lengths. This means that increases in debond and yield lengths with applied strain impair the efficiency of stress transfer across the interface, requiring longer distance from the fibre ends to reach the same level of stress than the fully bonded interface. Not only high values of τ_b and τ_{my} as shown in Fig. 9, but also a high frictional shear stress which is a product of the coefficient of friction and the residual fibre clamping stress improve the efficiency of stress transfer across the interface, giving rise to a shorter ineffective length [27].

4. Discussion and concluding remarks

In light of the parametric study made on carbon fibre composites containing epoxy and PEEK matrices for fully bonded, partially debonded and partially yielded interfaces, as presented in the preceding section, the sequence of failure process and the stress transfer phenomena can be highlighted which are most likely to take place in the fibre fragmentation test of single fibre model composites.

(1) At the initial stage of loading of microcomposites with an initial fibre length being sufficiently long (say, typically 50 mm), the fibre remains fully bonded with the matrix. The stress transfer across the fully bonded interface is insensitive to the interface properties, τ_b and τ_{my}, and is largely controlled by the elastic properties of the fibre and matrix.

(2) Once the maximum fibre axial stress reaches the local tensile strength, the fibre breaks. An increasingly higher external stress is required to fracture the fibres into smaller segments due to the dependence of the average fibre tensile strength on fibre length.

(3) Once the fibre fragment lengths become sufficiently short, interface failure (either debonding or matrix yielding depending on the relative magnitudes of interface bond strength, τ_b, and matrix shear yield strength, τ_{my}) occurs at the fibre ends. An increasingly

higher stress is required for the debond crack or matrix yielding to propagate towards the fibre centre. The interface shear stress becomes discontinuous at the boundary between the bonded and debonded interface regions.

(4) There are limits for the characteristic failed interface lengths before fibre fragmentation resumes. Interface properties, τ_b and τ_{my}, as well as the average fibre tensile strength, σ_{TS}, come to play a dominant role in determining the maximum debond and yield lengths for a given fibre length. A longer fibre length and higher interface properties, τ_b and τ_{my}, result in shorter maximum debond and yield lengths.

(5) A major difference between the composites with interface debonding and matrix yielding is that only a finite fibre length may be debonded from the brittle matrix due to the Poisson effect, whilst the whole fibre length may be yielded for ductile thermoplastic matrices when τ_{my} values are low.

(6) The critical transfer length can be determined based on the distribution of fibre fragment lengths which are obtained after a further substantial increment in the applied stress leads to no additional fibre fragmentation (provided that the matrix ductility is significantly greater than the fibre). The critical transfer length determined here consists of both bonded and failed interface lengths for a weak interface.

(7) The ineffective length for a fully bonded interface is constant, independent of external stress, given the properties of the composite constituents. Interface failure, whether brittle debonding or matrix yielding, degrades the efficiency of stress transfer as it continuously increases the ineffective length with increasing the external stress towards a maximum value. High interface properties both in the bonded and debonded regions are essential in promoting the stress transfer efficiency. A difference in the Poisson ratio between the fibre and matrix as discussed in the previous section and the geometric factors of the microcomposite, including the effective fibre volume fraction [8], are also an important factor determining the ineffective length for both fully bonded and failed interfaces.

The above description is essentially identical to what is normally observed in practical fibre fragmentation tests of single fibre composites with weak interfaces [13, 15, 20, 21, 25, 49, 50]. The observation of interface debond initiation at different stages of the fibre fragmentation processes reflects both the variation of fibre tensile strength and interface bond strength [21]. It has also been confirmed that the influence of various parameters including the strengths of the fibre, matrix and interface bond are highly dependent on the stage of failure process.

In the present model, transverse cracks of various shapes which propagate into the resin matrix depending on the nature of the interface bond and energy absorption capability of the matrix material have not been specifically taken into account. With a strong interface bonding and high matrix tensile strength, the transverse crack tends to be either penny-shaped or inclined cone-shaped. If the interface is strongly bonded and the matrix is weak in tension, a conical crack may propagate on the plane of principal stress [52, 53]. These matrix cracks are normally initiated from the broken fibre ends triggered by the energy suddenly released upon fibre fracture, and greatly affect the fracture of surrounding fibres in multiple fibre composites [54–58]. Debonding and matrix yielding at the interface region can relieve the stress concentration near the broken fibre ends which in turn discourages, to a certain extent, the propagation of transverse matrix cracks as shown in a study with specimens after hydrothermal ageing [49].

In addition, it is assumed here that only one of the two interface failure mechanisms, namely interface debonding or matrix yielding, can occur for a given combination of the fibre, matrix and interface properties. In other words, these failure mechanisms are assumed to be mutually exclusive. However, in reality, the interface failure may be a combination of debonding and matrix yielding in some polymer matrix composites. This is particularly true if the shear bond strength at the interface is more or less equivalent to the matrix shear yield strength. In matrix shear yielding, the effective thickness of the matrix material may be very small compared to the fibre diameter.

From the viewpoint of measuring the interface properties, there has hitherto been no systematic relationship developed between the experimental data obtained from the fibre fragmentation test and the useful interface properties, apart from the simple Kelly–Tyson [19] approach which has been widely employed. This can perhaps be attributed to the fact that there are too many unnecessary parameters involved in this test which need to be properly isolated in the data reduction scheme. The complications associated with the statistical nature of tensile strength of fibres due to the surface and internal flaws of random distribution are one example, and the difficulty associated with the characterization of the interface failure mechanisms another. For the fully bonded interface, none of the useful interface properties (e.g., interface shear bond strength, τ_b, at the bonded interface, and matrix shear yield strength, τ_{my}, coefficient of friction, μ, and residual fibre clamping stress, q_0, at the failed interface region) play a role in determining the critical transfer length or the ineffective length. As pointed out previously [51], the efficiency of stress transfer is simply controlled by the matrix mechanical properties rather than the interface properties if the apparent bond strength at the interface is sufficiently high (i.e., no debonding or matrix yielding). The linear dependence of the critical transfer length on Young's modulus ratio, E_f/E_m, in a ln–ln plot [39–41] testifies that there is little relevance of the parameters generated from the fibre fragmentation experiments with the interface properties. Further, unlike the fibre pull-out test [4, 5], the external load–strain curve does not render any indication of fibre fragmentation or interface failure. Simultaneous monitoring of acoustic events may only help to locate the fibre fragmentation.

The co-existence of bonded and failed interfaces in a broken fibre length for many composite systems does not render the direct extraction of meaningful interface properties directly from experiments. An

accurate measurement of the debond and yield lengths during the test may possibly provide information to establish the relationship between the interface properties at both the bonded and failed interfaces and the external stress. However such measurements have been difficult until the recent application of the laser Raman technique [14, 15] to the problem. However, once the fibre–matrix interface has failed the crack is unlikely to propagate in a stable way as is assumed in the model. The mixed mode failure, i.e., interface debonding versus matrix yielding, further complicates the interpretation of test data and requires detailed surface analyses.

The relationship between the number of broken fibres and the applied stress, whether the interface has failed or not, may only provide an indication of the efficiency of stress transfer. The specimen geometry and the loading conditions are not specifically designed to generate the desired information. The mode of failure process in this test may relate only indirectly to the interface properties that are the subject of investigation. Nevertheless, the interface parameters obtained in this test are shown to have intimate correlations with those from other micromechanical tests, and are used successfully to make valid comparisons between the composites containing fibres with varying prior surface treatments [59]. In summary, it may be rationalized that the significance of this test is to provide some measure of the relative stress transfer efficiency of different combinations of fibre, matrix and interface.

Appendix 1

$$D_1 = \frac{1 - \exp(-m_1 l)}{\exp(m_2 L)[\exp(-m_1 l) - \exp(-m_2 l)]} \quad \text{(A1)}$$

$$D_2 = -\frac{1 - \exp(-m_2 l)}{\exp(m_1 L)[\exp(-m_1 l) - \exp(-m_2 l)]} \quad \text{(A2)}$$

$$D_3 = -\frac{1}{\exp(m_2 L)[\exp(-m_1 l) - \exp(-m_2 l)]} \quad \text{(A3)}$$

$$D_4 = \frac{1}{\exp(m_1 L)[\exp(-m_1 l) - \exp(-m_2 l)]} \quad \text{(A4)}$$

and

$$m_1 = -\frac{B_1 + (B_1^2 + 4\lambda B_1)^{1/2}}{2} \quad \text{(A5)}$$

$$m_1 = \frac{-B_1 + (B_1^2 + 4\lambda B_1)^{1/2}}{2} \quad \text{(A6)}$$

where

$$B_1 = \frac{\alpha \nu_f + \gamma \nu_m}{\nu_m(\alpha + \gamma)} \frac{\beta_2}{\lambda} \quad \text{(A7)}$$

$$B_2 = -\lambda B_1 \quad \text{(A8)}$$

$$\frac{B_3}{B_2} = \frac{(1+\gamma)\nu_m}{\alpha \nu_f + \gamma \nu_m} \sigma + \omega \bar{\sigma} \quad \text{(A9)}$$

Also,

$$n_1 = \frac{-m_1 \exp(-m_1 l) + m_2 \exp(-m_2 l) + (m_1 - m_2)\exp[-(m_1 + m_2)l]}{\exp(-m_1 l) - \exp(-m_2 l)} \quad \text{(A10)}$$

$$n_2 = \frac{m_1 \exp(-m_1 l) - m_2 \exp(-m_2 l)}{\exp(-m_1 l) - \exp(-m_2 l)} \quad \text{(A11)}$$

$$n_3 = \alpha\lambda(\nu_m - \nu_f) + n_2(\alpha \nu_f + \gamma \nu_m) \quad \text{(A12)}$$

Appendix 2

(a) For a fully bonded interface
The stress ratio is:

$$\phi = \frac{\sigma_f(L-\delta)}{\sigma_f(0)_{L\to\infty}} = \frac{\cosh(\beta_2 L) - \cosh[\beta_2(L-\delta)]}{\cosh(\beta_2 L) - 1}$$

$$\simeq 1 - \cosh(\beta_2 \delta) + \tanh(\beta_2 L) \cdot \sinh(\beta_2 \delta)$$

$$\simeq 1 - \cosh(\beta_2 \delta) + [\cosh^2(\beta_2 \delta) - 1]^{1/2} \quad \text{(B1)}$$

since $\cosh(\beta_2 L) \gg 1$ and $\tanh(\beta_2 L) \approx 1$ for $L \to \infty$.

(b) For a partially debonded interface
The stress ratio is:

$$\phi = \frac{\sigma_f(L-\delta)}{\sigma_f(0)_{L\to\infty}} = \left[\left(\frac{1+\gamma}{\alpha+\gamma}\sigma - \frac{2\tau_b \cosh[\beta_2(L-\delta)]}{a\beta_2 \sinh[\beta_2(L-l)]}\right) \Big/ \left(\frac{1+\gamma}{\alpha+\gamma}\sigma - \frac{2\tau_b}{a\beta_2}\frac{1}{\sinh[\beta_2(L-l)]}\right)\right]$$

$$\simeq 1 - \frac{\alpha+\gamma}{1+\gamma} \cdot \frac{2\tau_b}{a\beta_2} \cdot \frac{1}{\sigma} \exp[\beta_2(l-\delta)] \quad \text{(B2)}$$

since $\sinh[\beta_2(L-l)] \approx \infty$ for $L \to \infty$.

(c) For a partially yielded interface
The stress ratio is:

$$\phi = \frac{\sigma_f(L-\delta)}{\sigma_f(0)_{L\to\infty}}$$

$$= \left[\left(\beta_2 l + \coth[\beta_2(L-l)] - \frac{\cosh[\beta_2(L-\delta)]}{\sinh[\beta_2(L-l)]}\right) \Big/ \left(\beta_2 l + \coth[\beta_2(L-l)] - \frac{1}{\sinh[\beta_2(L-l)]}\right)\right]$$

$$\simeq 1 - \frac{\exp[\beta_2(l-\delta)]}{\beta_2 l + 1} \quad \text{(B3)}$$

since $\cosh(\beta_2 L) \approx \sinh(\beta_2 L) \approx \cosh[\beta_2(L-l)] \approx \sinh[\beta_2(L-l)] \approx \infty$ for $L \to \infty$. Hence, half the ineffective lengths for the above three interface conditions are given in Equations 23–25.

Acknowledgements

The author wishes to thank the Research Grants Council (RGC) for the financial support of this work. Part of the paper has been presented at the 10th International Conference in Composite Materials (ICCM-10), Whistler, Canada, August 1995.

References

1. J. K. KIM and Y. W. MAI, *Compos. Sci. Technol.* **41** (1991) 333.
2. *Idem*, in "Structure and Properties of Fibre Composites, Materials Science and Technology", Vol. **13**, edited by T. W. Chou, (VCH Pub., Weinheim, Germany, 1993), pp. 239–289.
3. P. FELLIARD, G. DESARMOT and J. P. FAVRE, *Compos. Sci. Technol.* **50** (1994) 265.
4. L. M. ZHOU, J. K. KIM and Y. W. MAI, *J. Mater. Sci.* **27** (1992) 3155.
5. J. K. KIM, L. M. ZHOU, S. J. BRYAN and Y. W. MAI, *Composites* **25** (1994) 470.
6. J. K. KIM, L. M. ZHOU and Y. W. MAI, *J. Mater. Sci.* **28** (1993) 6233.
7. L. M. ZHOU, J. K. KIM, C. BAILLIE and Y. W. MAI, *J. Compos. Mater.* **28** (1995) 881.
8. J. K. KIM and Y. W. MAI, *J. Mater. Sci.* **30** (1995) 3024.
9. M. R. PIGGOTT, in "Load Bearing Fibre Composites" (Pergamon, Oxford, 1980) Ch. 4.
10. J. C. FIGUEROA, T. E. CARNEY, L. S. SCHADLER and C. LAIRD, *Compos. Sci. Technol.* **42** (1991) 77.
11. L. S. SCHADLER, C. LAIRD and J. C. FIGUEROA, *J. Mater. Sci.* **27** (1992) 4024.
12. J. DAOUST, T. VU-KHANH, C. AHLSTROM and J. F. GERARD, *Compos. Sci. Technol.* **48** (1993) 143.
13. L. DILANDRO, A. T. DIBENEDETTO and J. GROEGER, *Polym. Compos.* **9** (1988) 209.
14. H. J. GUILD, C. VLATTAS and C. GALIOTIS, *Compos. Sci. Technol.* **50** (1994) 319.
15. R. J. YOUNG and M. C. ANDREWS, *Mater. Sci. Engng* **A184** (1994) 197.
16. C. CAZENEUVE, J. E. CASTLE and J. F. WATTS, *J. Mater. Sci.* **25** (1990) 1902.
17. J. K. KIM, Y. W. MAI and B. J. KENNEDY, *ibid.* **27** (1992) 6811.
18. B. W. ROSEN, *AIAA Journal* **2** (1964) 1985.
19. A. KELLY and W. R. TYSON, *J. Mech. Phys. Solids* **13** (1965) 329.
20. F. C. LHOTELLIER and H. F. BRINSON, *Compos. Structures* **10** (1988) 281.
21. J. P. FAVRE, P. SIGETY and D. JACQUES, *J. Mater. Sci.* **26** (1991) 189.
22. R. GULINO, P. SCHWARTZ and S. L. PHOENIX, *ibid.* **26** (1991) 6655.
23. N. MELANITIS, C. GALIOTIS, P. S. TETLOW and C. K. L. DAVIES, *J. Compos. Mater.* **26** (1992) 574.
24. M. S. AMER, M. J. KOCZAK, C. GALIOTIS and L. S. SCHADLER, *Adv. Compos. Lett.* **8** (1994) 17.
25. M. DESAEGER, M. WEVERS and I. VERPOEST, Proceedings of ICCM-9, Madrid, Spain, edited by A. Miravete (Woodhead Pub., Cambridge, UK, 1993) pp. 732–739.
26. T. LACROIX, B. TILMANS, R. KEUNINGS, M. DESAEGER and I. VERPOEST, *Compos. Sci. Technol.* **43** (1992) 379.
27. J. IVENS, M. WEVERS and I. VERPOEST, *Composites* **25** (1994) 722.
28. L. T. DRZAL and M. J. RICH, in "Research Advances in Composites in the United States and Japan", ASTM STP 864, J. R. Vinson and M. Taya eds. (American Society for Testing and Materials, Philadelphia, PA. 1985) pp 16–26.
29. W. D. BASCOM and M. JANSEN, *J. Adhesion* **19** (1986) 219.
30. A. S. WIMOLKIATISAK and J. P. BELL, *Polym. Compos.* **10** (1989) 162.
31. G. MERLE and M. XIE, *Compos. Sci. Technol.* **40** (1991) 19.
32. E. K. DROWN, H. AL MOUSSAWI and L. T. DRZAL, *J. Adhesion Sci. Technol.* **5** (1991) 865.
33. A. DIANSELMO, M. L. ACCORSI and A. T. DIBENEDETTO, *Compos. Sci. Technol.* **44** (1992) 215.
34. B. YABIN, H. E. GALLIS, J. SCHERF, A. EITAN and H. D. WAGNER, *Polym. Compos.* **12** (1992) 329.
35. L. T. DRZAL and M. MADHUKAR, *J. Mater. Sci.* **28** (1993) 569.
36. T. OHSAWA, A. NAKAYAMA, M. MIWA and A. HASEGAWA, *J. Appl. Polym. Sci.* **22** (1978) 3203.
37. M. MIWA and N. HORIBA, *J. Mater. Sci.* **28** (1993) 6741.
38. M. MIWA and I. ENDO, *ibid.* **29** (1994) 1174.
39. C. GALIOTIS, R. J. YOUNG, P. H. J. YEUNG and D. N. BATCHELDER, *ibid.* **19** (1984) 3640.
40. EL. M. ASLOUN, M. NARDIN and J. SCHULTZ, *ibid.* **24** (1989) 1835.
41. Y. TERMONIA, *ibid.* **22** (1987) 504.
42. M. NARDIN and J. SHULTZ, *J. Mater. Sci. Lett.* **12** (1993) 1245.
43. *Idem*, *Compos. Interfaces* **1** (1993) 177.
44. L. MONETTE, M. P. ANDERSON and G. S. GREST, *J. Mater. Sci.* **28** (1993) 79.
45. L. MONETTE, M. P. ANDERSON, S. LING and G. S. GREST, *ibid.* **27** (1992) 4393.
46. J. M. WHITNEY and L. T. DRZAL, in "Toughened Composites", edited by N. J. Johnson ASTM STP 937 (American Society for Testing and Materials, Philadelphia, PA, 1987) pp. 179–196.
47. Y. LENG and T. H. COURTNEY, *Mater. Sci. Engng.* **A124** (1990) 141–149.
48. J. K. KIM and Y. W. MAI, *J. Mater. Sci.* **26** (1991) 4702.
49. Z. R. XU and K. H. G. ASHBEE, *ibid.* **29** (1994) 394.
50. C. L. SCHULTTE, W. McDONOUGH, M. SHIOYA, M. McAULIFFE and M. GREENWOOD, *Composites* **25** (1994) 617.
51. P. FELLIARD, G. DESARMOT and J. P. FAVRE, *Compos. Sci. Technol.* **49** (1993) 109.
52. J. V. MULLIN, J. M. BERRY and A. J. GATTI, *J. Compos. Mater.* **2** (1968) 82.
53. J. V. MULLIN and V. F. MAZZIO, *J. Mech. Phys. Solids* **20** (1972) 391.
54. H. D. WAGNER and L. W. STEENBAKKERS, *J. Mater. Sci.* **24** (1989) 3956.
55. S. L. PHOENIX, *Compos. Sci. Technol.* **48** (1993) 65.
56. H. STUMPF and P. SCHWARTZ, *ibid.* **49** (1993) 251.
57. K. D. JONES and A. T. DIBENEDETTO, *ibid.* **51** (1994) 53.
58. M. R. WISNOM and D. GREEN, *Composites* **26** (1995) 499.
59. P. J. HERRERA-FRANCO and L. T. DRZAL, *Composites* **23** (1992) 2.

Received 20 September 1995
and accepted 13 February 1996